Tuning photosensitized singlet oxygen production from microgels synthesized by polymerization in aqueous dispersed media

Luca Petrizza, Mickael Le Béchec, Emile Decompte, Hind El Hadri, Sylvie Lacombe-Lhoste, Maud Save

Tuning photosensitized singlet oxygen production from microgels synthesized by polymerization in aqueous dispersed media

Luca Petrizza, Mickael Le Bechec, Emile Decompte, Hind El Hadri, Sylvie Lacombe*, Maud Save*

CNRS/ Univ. Pau & Pays Adour/ E2S UPPA, IPREM, Institut des sciences analytiques et de Physicochimie pour l'environnement et les Matériaux, UMR5254, Hélioparc, 2 avenue Président Angot, 64053, PAU cedex 9, France

maud.save@univ-pau.fr

sylvie.lacombe@univ-pau.fr

† Electronic supplementary information (ESI) available.

Table of content entry

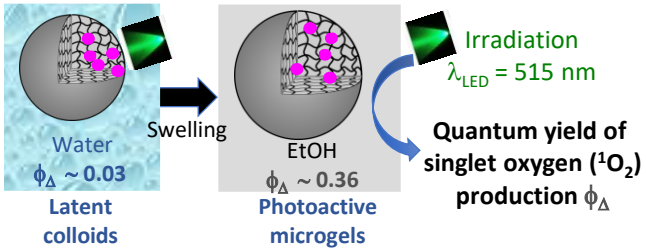

Miniemulsion copolymerization of vinyl acetate, *N*-vinylcaprolactam, vinyl benzyl Rose Bengal and divinyl adipate to synthesize switchable photosensitizer-grafted polymer colloids for interfacial photooxygenation reactions.

Abstract

Novel sub-micronic photoactive polymer colloids grafted with Rose Bengal (RB) photosensitizer were designed to promote singlet oxygen production from a supported organic photosensitizer. Photooxygenation of fine chemicals under visible light irradiation is considered as a green process. To enhance the overall process sustainability, stable colloidal particles were synthesized by polymerization in aqueous dispersed media with the ability to be transferred into ethanol, recycled by a centrifugation step and reused with no significant decrease of the quantum yield of singlet oxygen production. The microgels were synthesized for the first time by miniemulsion copolymerization of vinyl acetate (VAc), *N*-vinyl caprolactam (VCL), polymerizable vinyl benzyl Rose Bengal (VBRB) monomers and divinyl adipate (DVA) crosslinker. The microgels were characterized by UV-visible spectroscopy and compared with the homologue non-crosslinked polymer in order to discriminate the effect of RB grafted onto the linear polymer from its grafting inside crosslinked microgels. The quantum yields of singlet oxygen production were almost null in water but interestingly in the range of 0.27-0.47 in ethanol. The singlet oxygen quantum yield of these polymer materials is tuned by the aggregation state of VBRB units, hence producing an ON/OFF photosensitizing colloidal system. The absorption and emission spectra of the VBRB containing microgels in water were characteristic of strongly aggregated VBRB, while no evidence of aggregation was observed from the spectra in ethanol. The highest singlet oxygen quantum yield of the linear polymer was correlated with a less aggregated state of RB units compared with the crosslinked microgels. The present RB-based microgels were 20 % more resistant to photobleaching than free RB.

Introduction

Singlet oxygen production by photosensitization is a green chemistry process that takes advantage of oxygen from air as reactant and of visible light to excite a photosensitizer (PS). Singlet oxygen is a powerful selective oxidant, used for Photodynamic Therapy (PDT),[1–3] for the treatment/disinfection of environmental pollutants,[4,5] or for fine chemical synthesis.[6] The covalent grafting of PS onto polymer substrates has been extensively investigated as a strategy to transpose poorly soluble photosensitizers in solvent (or in water) while enhancing their stability and recycling. A large part of the literature is devoted to the field of PDT with studies describing multi-step syntheses of either star-like or block copolymers,[7–13] and the design of hydrogels.[14–16] It should be mentioned that the block copolymer self-assembly into micelles as nanoparticles dispersed in water required the systematic use of an organic co-solvent. On the other hand, photosensitizing polymer beads, mainly based on polystyrene and/or poly(vinyl benzyl chloride) polymers, with large diameters above 5 µm, have been extensively studied as support for interfacial production of singlet oxygen to promote photooxygenation reactions.[17–26] Polymer microbeads of 3–27 µm diameter were also prepared by thiol-ene photopolymerization and capped with C60 photosensitizer.[27] The singlet oxygen production mainly occurs at the surface of such large beads which are prone to sedimentation.

In the growing area of continuous-flow photochemistry implemented in microreactors for fine chemical oxidation,[28–31] a potential barrier to the use of the large photosensitizer-grafted polymer beads is their fast sedimentation rate and low specific surface area. It is thus important to develop a straightforward synthesis of stable submicronic polymer particles covalently grafted by an efficient organic photosensitizer.

Herein, we focus our attention on the covalent bonding of the Rose Bengal photosensitizer with the polymer to limit any catalyst leaching and to design robust organic photocatalysts suitable for photo-oxygenation of fine chemicals. Singlet oxygen is an elusive species with lifetime

depending on its surrounding medium (16 µs and 3.3 µs in ethanol and water respectively), so its diffusion length is highly dependent on the solvent.[6,32] At solid/liquid interface, singlet oxygen diffusion length is limited to several tens of nanometers.[33,34] Consequently, the reagents to be oxidized have to be in the vicinity of the photosensitizer to enhance the efficiency of the photosensitized oxygenation. Moreover, due to solubility issues, relevant photo-oxygenation reactions of fine chemicals such as α-terpinene or furfural have to be performed in organic solvents, among which alcoholic solvents are the less hazardous for any application.[6,35] To address these challenges, we describe here for the first time the synthesis of submicronic photosensitizing crosslinked colloidal particles by one pot miniemulsion copolymerization. These PS-grafted microgels are designed to exhibit swelling capacity in ethanol and should present several advantages: enhancement of reactant diffusion during the photooxygenation process, increase of the exchange surface due to their sub-micronic size, colloidal stability in the absence of sedimentation. Polymerizations in aqueous dispersed media (emulsion, miniemulsion, dispersion) are environmentally friendly processes of interest to synthesize stable dispersions of submicronic polymer colloids in one step in the absence of solvents.[36,37] Although polymer particles can be directly synthesized in alcoholic media by dispersion polymerization, this implies the choice of polymers that precipitate in alcohol preventing their swelling in ethanol. To the best of our knowledge, the development of polymer microgels with covalent anchoring of organic photosensitizer is very scarce. In parallel with the synthesis of crosslinked nanocapsules from sacrificial silica core embedding thionine photosensitizer, Shiraishi *et al.* described the synthesis of poly(*N*-isopropylacrylamide-*co*-vinyl benzyl chloride) microgels by precipitation polymerization, post-derivatized by thionine.[38] Sensitized oxygenation activity via the turnover number was estimated with the transformation of phenol to p-benzoquinone.[38] Lyon *et al.* synthesized Rose Bengal-grafted PNIPAM-based microgels with hydrodynamic diameter ranging between 90-600 nm, but the singlet oxygen production of

these colloids was not investigated at all.[39] Polyacrylamide hydrogel nanoparticles of 50-60 nm grafted with methylene blue were reported by Kopelman *et al.* for PDT purpose but the synthesis was performed by inverse microemulsion with 300 wt-% of surfactant versus monomers and hexane as organic continuous phase.[40]

In the present work, the commercially available Rose Bengal (RB) was selected as photosensitizer due to both its high value of singlet oxygen quantum yield in water (ϕ_Δ = 0.75) and ethanol (ϕ_Δ = 0.68-0.80)[41] and its reactivity towards vinyl benzyl chloride (VBC) to produce a polymerizable vinyl benzyl Rose Bengal (VBRB) monomer.[42,43] Statistical copolymerization of VBRB with *N*-vinylcaprolactam (VCL), vinyl acetate (VAc), and divinyl adipate (DVA) crosslinker is implemented to covalently anchor RB to the crosslinked latex particles during miniemulsion polymerization. The choice of P(VAc-*co*-VCL) copolymer to form the sensitizing colloidal particles was driven by its solubility in ethanol, thus conferring a swelling ability to the crosslinked particles compared with the more conventional polystyrene latex particles that do not swell in such solvent. Several studies have reported self-quenching of the photosensitizer induced by aggregation of the photosensitizer.[19,20,25,44–49] This will be taken as an advantage in the present work to design ON/OFF photosensitizing colloidal system by simple switching from water to ethanol. Here, we aim to provide a detailed study on singlet oxygen production via the measurement of the singlet oxygen quantum yield ($\emptyset_\Delta$). This allows an accurate comparison of the singlet oxygen production between the different systems (free rose Bengal, linear and crosslinked P(VAc-*co*-VCL-*co*-VBRB) polymer), independently from the RB concentration.

Experimental section

Materials.

4-vinylbenzyl chloride (VBC, 90 %), Rose Bengal (RB, 95 %), *N*,*N*-Dimethylformamide (DMF, 99.8 %), acetone (99.9 %), chloroform (99 %), methanol (99.8 %), diethyl ether (99.8 %), vinyl acetate (VAc, 99 %), N-vinylcaprolactam (VCL, 98 %), 2,2-azobis(2-methylpropionitrile) (AIBN, 98 %), 1,3,5-trioxane (TR, 99 %), furfuryl alcohol (FFA, 99 %), ethanol (for UV spectroscopy, 96 %), 1,3-diphenylisobenzofuran (DPBF, 97 %), 1,3,5-trioxane and hexadecane (HD, 99 %) were purchased from Sigma-Aldrich Co. (St Louis, USA). Divinyl adipate (DVA, ≥99 %) was purchased from TCI Europe N.V. (Paris, France). Dimethyl sulfoxide-d_6 (99.8 %) was purchased from Euriso-Top Sas (Saint-Aubin, France). Sodium dodecyl sulfate (SDS, 99 %) was purchased from ABCR GmbH (Karlsruhe, Germany). Sodium bicarbonate (SbC, $NaHCO_3$, 99 %) was purchased from VWR International S.A.S. All the purchased chemicals were used as received except furfuryl alcohol, freshly distilled (boiling point 170°C) before use. ALUGRAM® aluminium sheets SIL G/UV254 for TLC were purchased from MACHEREY-NAGEL GmbH & Co (Düren, Germany). Dialysis was performed against water at room temperature under gentle stirring with Spectra/Por® Dialysis membrane (Spectrum Laboratories, Inc., Rancho Dominquez, USA, mol wt cutoff >3.5 kDa, average diameter 33 mm).

Characterization methods.

NMR spectra were recorded using a Brüker 400 MHz spectrometer at 25 °C. ^{1}H measurements were performed at 400 MHz and ^{13}C measurements at 100 MHz.

The hydrodynamic diameter (D_h) of the microgels were measured by Dynamic Light Scattering (DLS) using a Malvern Nano ZS instrument equipped with a He-Ne mW power laser operating at a wavelength of 633 nm. Dialyzed samples were housed in disposable polystyrene cuvettes of 1 cm optical path length, using double deionized water or ethanol as solvent, at 25° C and at a concentration of 0.05 g L^{-1}. The width of the hydrodynamic diameter distribution is provided

by the Cumulant analysis and reported as the Polydispersity Index (PDI). D_h values reported in **Table 1** were calculated from the intensity of light scattered by particles (10 measurements per sample) from a multiple narrow mode (non-negative least squares (NNLS) analysis) to obtain the particle size of each population.

The MG and VBRB@MG microgels were also analyzed by asymmetrical flow field-flow fractionation (AF4) running with aqueous eluent. An Eclipse 3+ AF4 instrument (Wyatt Technology, Dernbach, USA) equipped with a 1200 series high-performance liquid chromatography pump (Agilent Technologies, Les Ulis, France) was used as a separation system. All injections were performed with an Agilent Technologies 1260 ALS series autosampler. The detection system was formed by a 1200 series UV-vis absorbance detector (Agilent Technologies) and a multi-angle laser light scattering (MALLS) detector (DAWN HELEOS, Wyatt Technology). The AF4 channel thickness was fixed by a 250-µm Mylar spacer (with dimensions of 26.5 cm length and narrowing width from 2.1 to 0.6 cm). The accumulation wall was defined by a 10-kDa polyethersulfone (PES) membrane purchased from Wyatt Technology. The AF4 conditions used in this study were: an elution flow rate of 0.5 mL min^{-1}, an injection flow rate fixed at 0.2 mL min^{-1}, a focus flow rate of 0.5 mL min^{-1} and a cross flow rate (decreasing exponential) of $2e^{-0.27t}$ mL min^{-1} (with t the time).[50,51] The mobile phase was prepared with sodium nitrate ($NaNO_3$) diluted in deionized water (to reach a concentration of 0.5 mmol L^{-1}) and filtered at 0.1 µm. The overlay of the UV-visible trace recorded at 559 nm, characteristic absorption wavelength of Rose Bengal derivatives, with light scattering trace confirms the presence of VBRB inside the microgels. The gyration radius (R_g) was measured from the plot of scattered light intensity versus the wave vector ($q = (4\pi/\lambda) \sin\theta/2$) using the sphere model with ASTRA software (version 6, Wyatt technology). The polymer concentration was set at 5 mg L^{-1}.

TEM images were recorded on a TEM JEOL JEM 1400 with a tungsten filament working at 120KeV, an objective diaphragm to improve the contrast and a Gatan Orius 1000 camera. The samples dispersed in water were casted onto TEM grids.

Photophysical measurements.

UV-VIS absorption spectra were recorded at 5, 10 and 25 °C by means of Perkin-Elmer Lambda 850 spectrophotometer. Corrected steady-state emission and excitation spectra were recorded with a photon counting Edinburgh FLS920 fluorescence spectrometer equipped with Xe lamp. The concentrations of all compounds were adjusted to give an absorbance around 0.1 at the absorption maximum. Quartz cuvettes (Hellma) with optical path length of 1 cm were used for both absorbance and emission measurements. The detailed irradiation experiments and equations used for singlet oxygen quantum yield determination, photobleaching and cycling photooxygenation measurements are described in Electronic Supplementary Information.

General procedure for the synthesis of crosslinked particles and linear polymer by miniemulsion polymerization. The synthesis of the VBRB monomer is described in Electronic Supplementary Information (Fig. S1†) and the corresponding ^{1}H,^{13}C NMR and UV spectra are displayed in Fig. S2†, Fig. S3† and Fig. S4†. The microgels were synthesized by miniemulsion polymerization carried out at 10 wt% of initial solid content. The organic phase containing VAc, VCL, TR, AIBN, HD, DVA and VBRB was stirred at 0°C for 15 min. The aqueous phase consisted of SDS and SbC, dissolved in double deionized water (DW) and was stirred at room temperature for 30 min and thus sonicated with an ultra-probe VIbraCell 72408, Bioblock Scientific in a continuous mode (power 30 % for 6 min). The organic phase was added to the aqueous phase and stirred at 0°C for 15 min. The reaction mixture was introduced in a 100 mL round bottom flask equipped with a stirring bar set at 300 rpm and purged with a gentle flow of

nitrogen at 0°C for 30 min. The round bottom flask was placed into an oil-bath previously heated to 65 °C and the reaction mixture was stirred for 3 h, then cooled to room temperature and oxygen was introduced in the reaction mixture. The recipes for the microgel syntheses are reported in Table S1. The final monomer conversion calculated by ^{1}H NMR (See Fig. S5† and S6†) ranged from 50 to 90 %. The final microgels were dialyzed in DW at room temperature for 48 h. The codes MG-*w* correspond to the initial weight fraction (*w*) of DVA crosslinker used in the synthesis of microgels (MG), calculated on the basis of the mass of crosslinker and VAc/VCL monomers: $w = m_{DVA}/(m_{DVA} + m_{VCL} + m_{VAc})$. In order to assess the ability of the photoactive microgels to be separated from the reaction medium while being still photoactive, the VBRB@MG-14 microgels were centrifuged at 4°C, 10 000 g on a Beckman Coulter Aventi J30I centrifuge.

Results and discussion

Synthesis and colloidal characterization of photosensitizing polymer colloids.

Due to the aromatic structure of RB, the derived VBRB vinyl monomer is poorly soluble in water. Contrary to emulsion polymerization which requires monomer diffusion through the aqueous continuous phase, miniemulsion is advantageous to disperse highly hydrophobic species as the particle nucleation proceeds in the monomer droplets formed by shearing the initial dispersed phase.[36] The choice of the VCL and VAc monomers was driven by different parameters that were not achievable by using more conventional styrene or alkyl (meth)acrylate monomers, widely used in miniemulsion polymerization. First, the mixture of VAc and VCL was able to solubilize VBRB, otherwise almost insoluble in *n*-butyl acrylate or methyl acrylate for instance. The best organic solvent for RB derivatives is dimethyl formamide (DMF) and VCL is an amide, liquid at temperature above 35-38°C, with good solubilisation capacity towards VBRB. Secondly, VAc and VCL are sufficiently hydrophobic (($[VCL]_{limit, water, 25°C}$ =

41 g L^{-1}, $[VAc]_{limit,\ water,\ 20°C}$ = 23 g L^{-1})[52,53] to promote the formation of monomer droplet at 10 wt-% (*ie* 100 g.L^{-1}) of initial monomer content in water. Vinyl acetate enables the solubilisation of the solid VCL to form the initial monomer droplets at room temperature while being efficiently copolymerized with VCL,[54–56] which avoids the use of an organic co-solvent that should be removed at the end of polymerization as reported by Crespy *et al*..[57] In the present work, the P(VAc-*co*-VCL)-based particles were synthesized by miniemulsion polymerization in the presence of hydrophobic hexadecane limiting the Ostwald Ripening, as depicted in Scheme 1.[36]

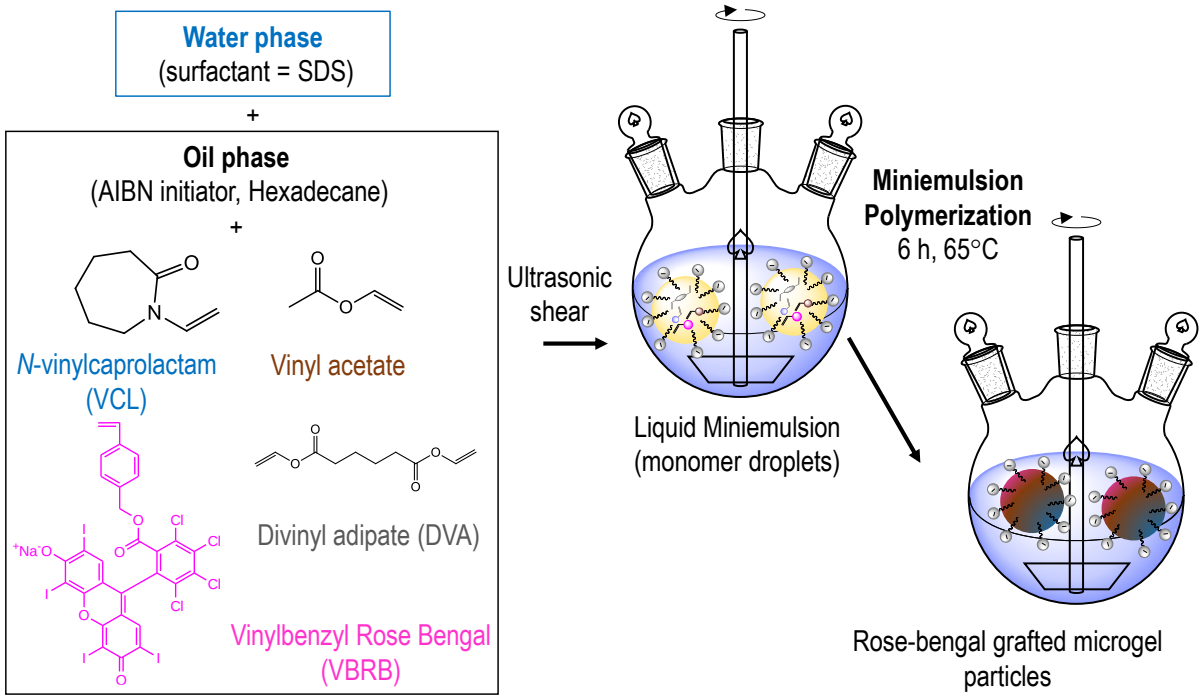

Scheme 1 : Reaction scheme for the synthesis of photosensitizing microgels by miniemulsion copolymerization.

A series of four microgels were synthesized (Figure 1): *i)* two model photosensitizer-free microgels crosslinked with 8 or 14 mol % of the divinyl adipate (DVA) crosslinker (MG-8, MG-14 in Table 1), and *ii)* two homologue microgels containing Rose Bengal photosensitizer synthesized by miniemulsion copolymerization of 0.6 mol-% of VBRB (ie 5.6 wt %, initial loading 50 µmol g^{-1}) based on the total number of moles of VAc, VCL and DVA (VBRB@MG-

8, VBRB@MG-14 in Table 1). In order to discriminate the effect of RB grafting onto P(VAc-*co*-VCL) copolymer from the effect of the microgel environment on photoactivity, a linear P(VAc-*co*-VCL-*co*-VBRB) was synthesized by miniemulsion copolymerization in the absence of DVA crosslinker (VBRB@P in Table 1).

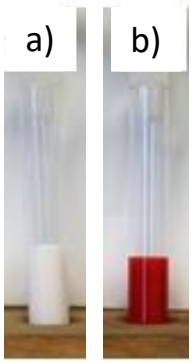

Figure 1. Pictures of the final polymer dispersions in water obtained by miniemulsion copolymerization of VAc and VCL (Table 1): a) MG-8; b) VBRB@MG8.

Table 1. Characterization of the microgels: RB loading, hydrodynamic diameter D_h in water and alcohol, gyration radius R_g, singlet oxygen quantum yields ϕ_Δ in water and alcohols.

Expt	$D_{h,\,H20}$ (nm) [a] (PDI)	$D_{h,\,EtOH}$ (nm) [a] (PDI)	SR [b]	$R_{g,H20}$ [c] (nm)
MG-8	190 (0.05)	247 (0.06)	2.2	90
MG-14	171 (0.06)	205 (0.03)	1.7	80
VBRB@MG-8	262 (0.16)	285 (0.44)	1.3	100
VBRB@MG-14	241 (0.17)	260 (0.31)	1.3	100

[a] Hydrodynamic diameter (D_h) values and polydispersity index measured in water or ethanol for [microgel] =0.05 g L^{-1} ; [b] Swelling ratio, SR = $R_h^3{}_{EtOH}$ / $R_h^3{}_{H20}$, where R_h is the hydrodynamic radius at 25° C; [c] Gyration radius measured by MALLS.

The P(VAc-*co*-VCL) microgels were synthesized by miniemulsion polymerization up to complete monomer conversion within 3 hours. Stable microgels dispersed in the aqueous phase

exhibit a narrow particle size distribution (PDI < 0.1, see MG-8 and MG-14 in Table 1 and Fig. S7†). Miniemulsion process requires the addition of a hydrophobic molecule (hexadecane in the present work) in order to limit the monomer diffusion through the water phase which would results in larger droplets at equilibrium.[36,58] The higher Laplace pressure of small droplets should be counterbalanced by the non-favorable increase of the osmotic pressure in case of increasing hexadecane concentration through monomer exit. The RB-free microgel crosslinked with 8 mol-% of DVA (MG-8) displays an average hydrodynamic diameter (D_h) of 190 nm, slightly higher than the microgels crosslinked with 14 mol-% of DVA (D_h = 171 nm for MG-14 in Table 1**)**. A similar trend was observed for the RB-grafted microgels as 10 % of D_h decrease was observed by increasing the initial crosslinker ratio from 8 mol-% to 14 mol-% (see VBRB@MG-8, and VBRB@MG-14 in Table 1). It should be mentioned that all microgels dispersed in water are stable over months in the absence of sedimentation. The copolymerization of VBRB induced an increase of D_h measured in water (see MG-8 *vs* VBRB@MG-8 and MG-14 *vs* VBRB@MG-14 in Table 1). The VBRB monomer introduces ionic moieties inside the polymer network (see scheme 1). The ionic contribution to the total osmotic pressure is known to enhance microgel swelling.[59] The characterization of the VBRB@MG-8 microgels by TEM revealed a different contrast in the VBRB@MG microgels compared to the RB-free counterparts (Figure 2), which probably highlight the presence of the heavy iodide atoms in RB moiety.

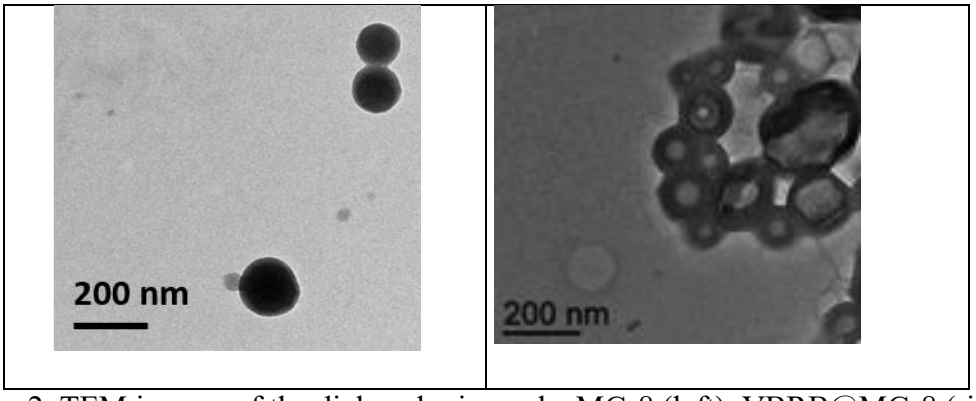

Figure 2. TEM images of the dialyzed microgels: MG-8 (left), VBRB@MG-8 (right).

The dialyzed microgels were also analysed by Asymetrical Flow Field-Flow Fractionation (AF4) equipped with UV-visible detector set at a wavelength of 559 nm, a characteristic wavelength of RB moiety compared to the polymer, and a MALLS detector. As depicted in Figure 3, the absorbance traces of VBRB@P and VBRB@MG-8 samples overlay with the light scattering (LS) traces which supports the presence of VBRB within the colloids. It should be noted that the colloidal dispersion scatters light which induces an extra-absorbance at 559 nm due to the slight upper shift of the baseline of UV-visible spectra for all the microgels (see Fig. S8†). However, at a concentration of 5 ppm, the ratio between the areas of the LS signal over the UV-visible signal is 5 times higher for VBRB@MG-8 microgel than for the MG-8 microgel (Table S2). This confirms that the UV-visible trace at 559 nm arises mainly from the VBRB units.

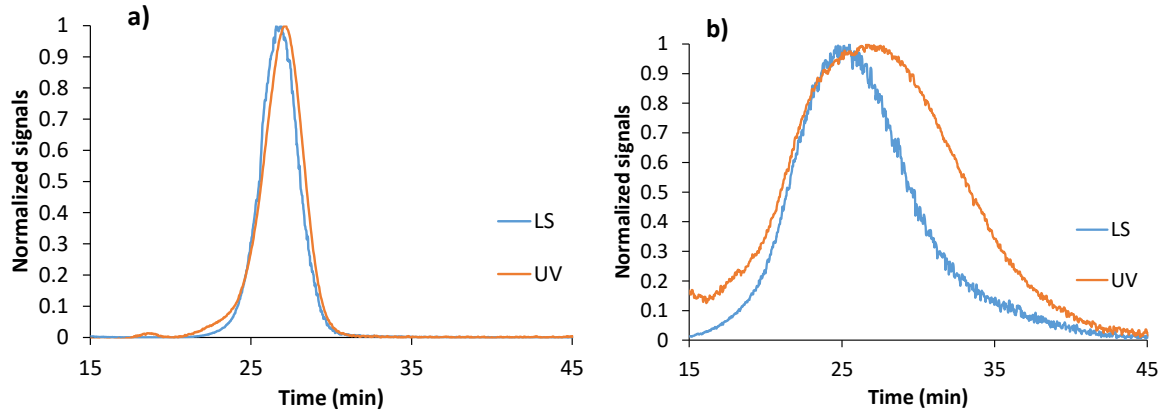

Figure 3. A4F fractograms in $NaNO_3/H_2O$ eluent of: a) VBRB@P and b) VBRB@MG-8. Overlay of the light scattering (LS, orange) and UV-visible (λ = 559 nm, blue) traces.

The microgels were dried to be further dispersed in ethanol, a solvent suitable for photooxygenation reactions of organic molecules of interest such as α-terpinene or furfural.[6,35] Interestingly, both MG and VBRB@MG crosslinked microgels had the ability to swell in ethanol as shown by the higher D_h value measured in ethanol than in water (**Table 1**). The lower swelling ratio of the VBRB@MG compared to MG is due to the higher diameter in water as

discussed above. The swelling ability of microgels is of high interest to increase the diffusion of oxygen in the vicinity of the grafted photosensitizer.

Characterization of the photophysical properties of the polymer colloids.

In order to correlate the swelling ability of the microgels to the yield of singlet oxygen production, the singlet oxygen quantum yield (ϕ_Δ) was monitored in both water and ethanol. The singlet oxygen quantum yield, corresponding to the number of moles of singlet oxygen produced per photon adsorbed by the photosensitizer, will be measured using two different quenchers, either furfuryl alcohol (FFA) in water or diphenylisobenzofuran (DPBF) in ethanol (Scheme 2). The oxidation of FFA to 6-hydroxy-(2H)-pyranone is monitored by HPLC, while DPBF concentration is calculated from the decrease of its absorbance spectra at 410 nm. The oxidation of FFA follows a pseudo first order kinetics (see Eq. 4 in Electronic Supplementary Information), while the decrease of DPBF followed a more general kinetic scheme (see Eq.5 in Electronic Supplementary Information).

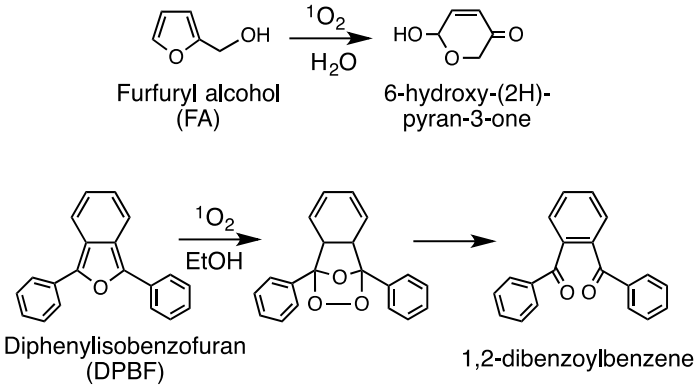

Scheme 2. Singlet oxygen quenching by FA in water and by DPBF in ethanol

Prior to measurement of the quantum yield of singlet oxygen production, it is important to carefully analyze the UV-visible absorbance and emission spectra of the different materials. Both absorption and emission spectra of the synthesized VBRB monomer were recorded in

ethanol (see Fig. S4†). The maximum absorbance and emission wavelengths (λ_{abs}= 559 nm, λ_{em}= 573 nm) as well as the shoulder peak at 514 nm were slightly red-shifted relative to free RB ($\lambda_{abs,max}$ = 548 nm, $\lambda_{em,max}$ = 569 nm) as already reported for other aromatic derivatives of RB.[60] This confirms the successful nucleophilic substitution of Rose Bengal with vinyl benzyl chloride to produce a pure styrenic monomer. The absorbance and emission spectra of both the RB-grafted microgels (VBRB@MG) and the non-crosslinked copolymer (VBRB@P) dispersed in water are displayed Figure 4. First, we can notice that the adsorption bands of the VBRB@P linear polymer are broader than those of free RB with a red-shifted maximum at 565 nm, an intense shoulder at 535 nm and a weak band at 428 nm. It has been previously reported that dimers of RB ethyl esters in water were characterized by two absorption bands at 526 and 572 nm.[61] The absorbance spectrum of the linear polymer VBRB@P (Figure 4), with a noticeable decrease of the I_{565}/ I_{535} intensity ratio relative to the I_{548}/ I_{514} ratio in Rose Bengal, and the broadening of the absorption bands,[62] both support the assumption of slight aggregation of VBRB moiety in the VBRB@P polymer dispersed in water. This is in agreement with our previous results showing that amphiphilic P(VAc-*co*-VCL) statistical copolymer chains with 50/50 composition in VAc/VCL slightly self-assembled via hydrophobic interactions, even below the phase transition temperature (PTT ~ 17-20 °C) of these copolymers in water.[52,53] The UV spectra of the linear VBRB@P polymer in water exhibit the characteristic traces of RB aggregation even at low temperature (5 °C and 10 °C) (Fig. S9†). The same P(VAc-*co*-VCL) copolymers crosslinked with the hydrophobic DVA are likely in a more collapsed state within the colloidal particles as the microgels do not exhibit any swelling-to-collapse transition in water over the all temperature range from 10 to 50 °C (Fig. S10†). This collapsed state induces an intense distortion of the absorption spectra of the grafted RB moieties in the VBRB@MG microgels (Figure 4). Figure 4 displays absorption spectra in which the drift of the baseline arising from the light scattered by the dense particles has been corrected (see raw data in Fig.

S8†). A very broad band is observed for both VBRB@MG-8 and VBRB@MG-14 microgels, with a maximum absorbance at 544 nm and prominent shoulders on the high energy side at 518 nm and 436 nm (this latter noticeably more intense than in VBRB@P) and on the low energy side at 576 nm. The spectra of these microgels are more difficult to rationalize since their shapes are indicative of optically thick samples strongly modified by diffusion effects. Higher dimer/monomer ratio in the cross-linked microgel can however be assumed.

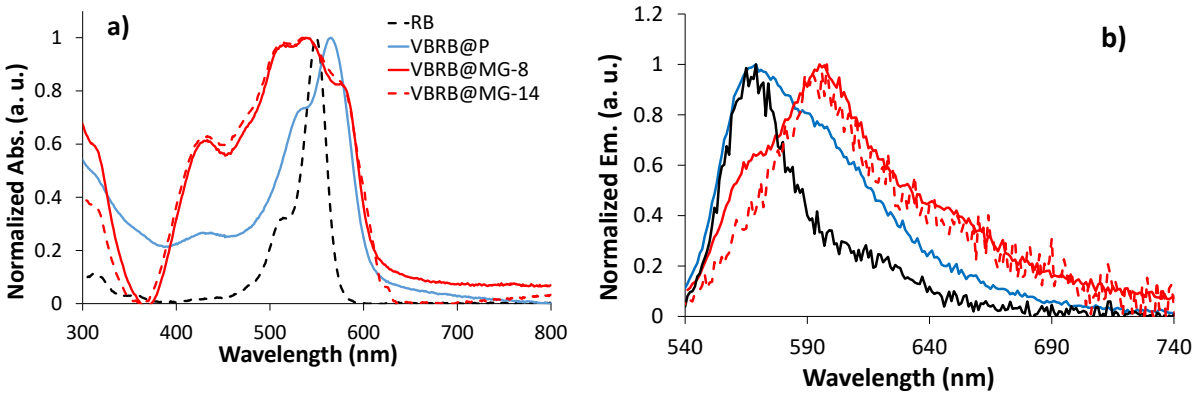

Figure 4: a) Normalized absorption spectra b) emission spectra (λ_{ex} 530 nm) in H_2O of the soluble polymer VBRB@P (blue lines), microgels VBRB@MG-8 (continuous red lines), VBRB@MG-14 (dotted red lines), polymer concentration in H_20 [13.0 mg L^{-1}] together with RB spectra in H_2O [1.0 µM] (black lines).

The emission spectrum of VBRB@P (λ_{em} = 569 nm) (Figure 4b) is similar to that of free RB but exhibits a broader signal compared to the emission spectrum of free RB, as expected for aggregated species. On the contrary, the emission spectra of VBRB@MG-8 and VBRB@MG-14 microgels in water show a bathochromic shift (λ_{em} 595 nm) relative to free RB (λ_{em} 569 nm) and a growing shoulder at longer wavelengths typical of inner filter effects,[63] with reabsorption of the 0-0 emission band, indicative of strong aggregation in this optically thick sample. Additionally the fluorescence excitation spectra are expected to be different from the absorption spectrum for a solution containing monomeric photosensitizer and its aggregates absorbing in the same region.[64] This is actually observed for the VBRB@P linear copolymer

and VBRB@MG-8, VBRB@MG-14 microgels in water (Fig. S11†). To summarize these spectral data, aggregation of RB units is observed for the different RB-grafted polymers dispersed in water and this aggregation is much more significant in the crosslinked microgels than in the corresponding linear soluble polymer.

It is worth noting that the aggregation of RB moieties in the linear or crosslinked P(VAc-*co*-VCL-*co*-VBRB) dispersed in water is correlated to very low values of singlet oxygen quantum yields ($0.01 < \phi_{\Delta} < 0.05$, Table 2). Thus, the synthesis of VBRB@MG microgels by polymerization in aqueous dispersed media (miniemulsion polymerization) produces "latent" microgels which are not photo-active in water under light irradiation at 515 nm due to the aggregated state of RB moieties in the collapsed polymer. In relationship with their respective solubility and swelling ability in ethanol, the photosensitized linear copolymer and microgels were further dispersed in ethanol to monitor their propensity to produce singlet oxygen. Note that VBRB, which is soluble in ethanol up to 0.05 mol L^{-1}, is as efficient as free RB to produce singlet oxygen in ethanol (see Table 2, $\phi_{\Delta} = 0.72$). In ethanol, the absorbance and emission spectra of the RB-grafted copolymers are very close to that of the free VBRB monomer in the same solvent (Figure 5) and strikingly different from their spectra in water (Figure 4a and b).

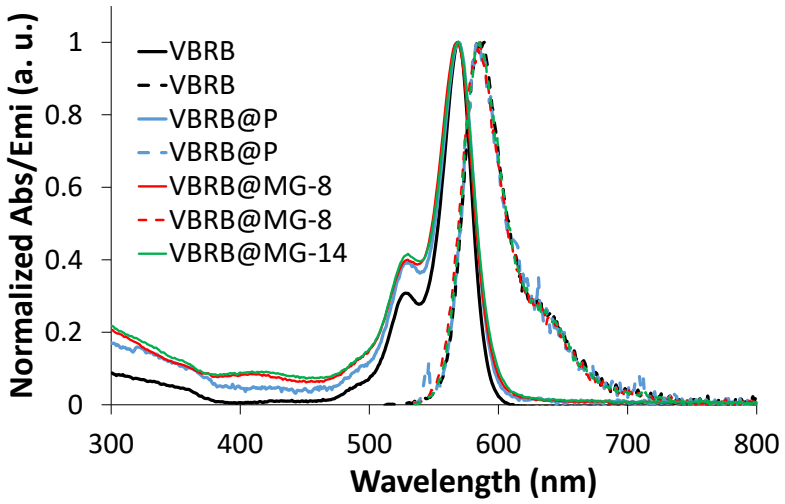

Figure 5. Normalized absorption (full lines) and emission (dotted lines, λ_{ex} 530 nm) spectra in ethanol of VBRB ([VBRB] = 0.98×10^{-6} M) and VBRB@P, VBRB@MG-8, VBRB@MG-14 at polymer concentrations ranging from 0.003 to 0.007 g L^{-1}.

Moreover, the extent of crosslinking had no influence on the spectra, as the patterns of VBRB@P, VBRB@MG-8 and VBRB@MG-14 perfectly overlaid. It can be also noticed that the absorption and excitation spectra of RB-based soluble linear polymer and dispersed microgels perfectly matched (Fig. S12†). All these spectral features tend to show that the RB moieties do not aggregate inside the swollen microgels in ethanol, contrary to the strong aggregation observed in the collapsed state of the microgels dispersed in water. The three types of RB-grafted polymeric materials proved to be photoactive in ethanol producing singlet oxygen under irradiation. Indeed, the singlet oxygen quantum yields (ϕ_Δ) ranged between 0.47 and 0.32 for VBRB@P and VBRB@MG (Table 2), the highest value being obtained with the soluble VBRB@P linear polymer. These values are rather high for supported Rose Bengal.[62] The efficiency of the VBRB@MG in producing singlet oxygen in ethanol can thus be ascribed to the absence of any aggregation of the covalently grafted RB in the swollen microgels. We can conclude that the latent non-photoactive VBRB@MG polymer colloids dispersed in water were turned ON into very active systems in ethanol. It is well known from the literature that the singlet oxygen production is drastically reduced by the photosensitizer aggregation, which enhances self-quenching of the excited state,[44,25] as demonstrated for instance with lipophilic phthalocyanines included in polymer hydrogels of various lipophilicity.[65] Aggregation effects, were also reported to be responsible for the decrease of singlet oxygen quantum yield of either RB esters insoluble in non-polar solvents[66] or RB-grafted to poly(styrene-*co*-vinylbenzylchloride) beads.[67]

It should be noticed that VBRB@MG-14 microgels were centrifuged to assess the recovery of the supported photosensitizer separately from the photo-oxidized molecules. This recycling step is expected to minimize the tricky distillation steps usually applied to recover from the solvent the oxidized product free of photosensitizer. Centrifuged VBRB@MG-14 microgels were mixed with DPBF in ethanol to be further irradiated by the LED at 515 nm. The VBRB@MG-

14 were still photoactive after the centrifugation cycle with a singlet oxygen quantum yield in a similar range (ϕ_Δ = 0.32).

Table 2. Singlet oxygen quantum yields ϕ_Δ of free RB, VBRB and dialyzed polymers.

Expt	ϕ_Δ (H_2O)[a]	ϕ_Δ (EtOH) [b]
Free RB	0.75	0.68-0.80 [c]
		0.75
VBRB	-	0.72
VBRB@P	0.05	0.47
VBRB@MG-8	0.03	0.27
VBRB@MG-14	0.01	0.35

[a] Singlet oxygen quantum yields measured in water with FFA quencher (LED at 515 nm, irradiance of 3 mW cm^{-2}); [b] Singlet oxygen quantum yields measured in ethanol with DPBF quencher (Xe-Hg Lamp Monochromator 547 nm, irradiance of 0.2 mW cm^{-2}); [c] Extracted from reference [41].

The reusability of VBRB@MG14 microgels was investigated through a repeated use of the photosensitized colloids in five photooxygenation cycles. The overlay of the DPBF conversion versus time for each cycle reveals that the high efficiency is maintained over the different cycles (Figure 6a) while no DPBF conversion could be detected in the dark. It is worth noting that under the conditions used for singlet oxygen measurement in ethanol at low irradiance (0.2 mW cm^{-2}), neither RB nor VBRB@MG photobleached (constant absorbance at λ 569 nm). In order to highlight the interest of RB grafting, free RB and VBRB@MG-14 were irradiated in ethanol with a more powerful Xenon lamp (irradiance 55 mW cm^{-2}) to allow the comparison of their photobleaching yield (see Eq. 1 in the experimental part). The VBRB@MG-14 microgels were

more photo-stable (36 % photobleaching) than free RB (53 % photobleaching) over 6 hours of intense irradiation (Figure 6b). It should be noted that the photo-stability of VBRB@MG14 particles is maintained over more than 12 months with very close value of singlet oxygen quantum yield (Table S3).

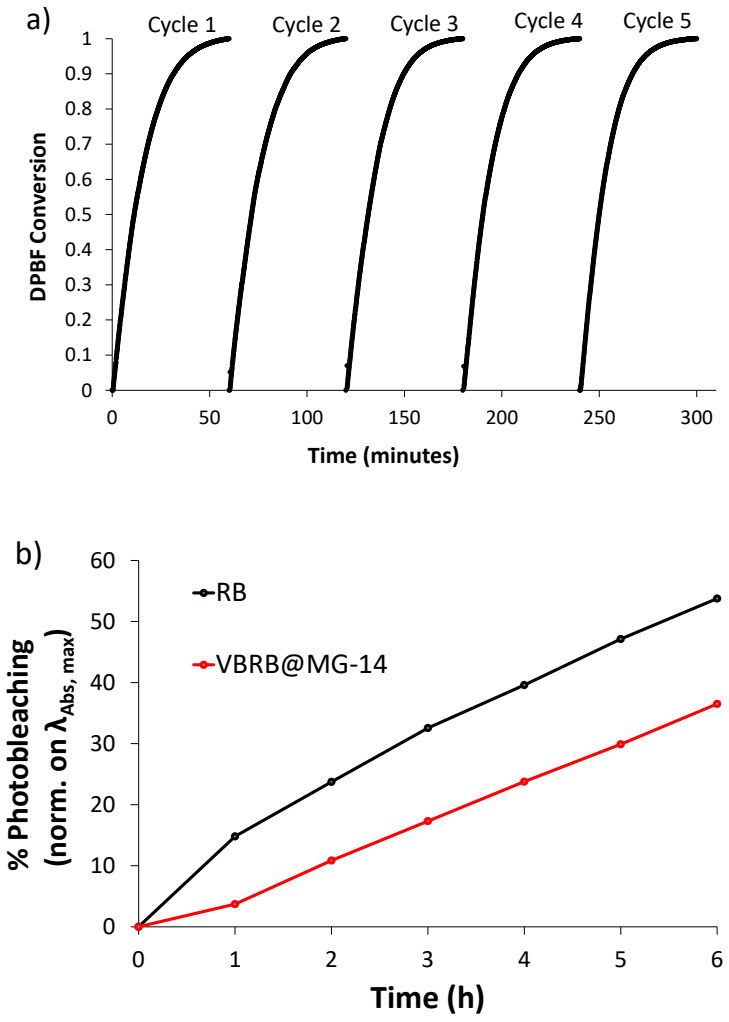

Figure 6 : a) Five photooxygenation cycles of DPBF from VBRB@MG-14 (Xe-Hg Lamp Monochromator 547 nm, irradiance of 0.2 mW cm^{-2}); b) Comparison of the rate of photobleaching of RB and VBRB@MG-14 in ethanol (300 W Xe Lamp, Irradiance 55 mW cm^{-2} between 400 and 800 nm).

Conclusions

In conclusion, novel photosensitizer-grafted polymer colloids of submicronic diameter were designed as efficient tool to trigger the photoactivity of supported Rose Bengal. Interestingly, the Rose-Bengal microgels were synthesized by a one-step miniemulsion copolymerization of vinyl benzyl rose Bengal, vinyl acetate, *N*-vinyl caprolactam and divinyl adipate crosslinker carried out in aqueous dispersed media. We designed a switchable system via the synthesis of non-photoactive latent polymer colloids in water which can be triggered into photoactive particles in ethanol with a good level of singlet oxygen quantum yield (ϕ_Δ = 0.32-0.47) via Rose Bengal disaggregation through simple swelling of these microgels. Their photo-activity is maintained after 5 repeated use of the photosensitized microgels in photooxygenation cycles but also after their centrifugation, which opens perspectives towards an efficient separation of the supported sensitizer from the reaction medium. The reusability and recyclability of the organic photocatalyst limiting any distillation step is will increase the sustainability of the catalytic photooxygenation green process. The switchable photo-activity represents an advantage as latent photoactivity in water during storage should enhance the photostability while efficient photoactivity in ethanol is of particular interest to trigger photo-oxygenation reactions. These original sub-micronic microgels open the route towards further implementation of fine chemicals photooxygenation in flow photoreactors, in the absence of substrate sedimentation.

Conflicts of interest

There are no conflicts to declare.

Acknowledgements

The authors would like to thank Agence Nationale de la Recherche (ANR) for funding PICPOSS project (ANR-15-CE07-0008-03), CNRS and UPPA for financial support. The authors would like to thank Abdel Khoukh, Elise Deniau and Bruno Grassl (UPPA) for their

support respectively in NMR, DLS and A4F techniques and Armel Descamps-Mandine Center of Micro-characterization Raimond Castaing, Toulouse) for the TEM images.

Notes and references

1 S. S. Lucky, K. C. Soo and Y. Zhang, *Chem. Rev.*, 2015, **115**, 1990–2042.

2 Z. Zhou, J. Song, L. Nie and X. Chen, *Chem. Soc. Rev.*, 2016, **45**, 6597–6626.

3 W. Fan, P. Huang and X. Chen, *Chem. Soc. Rev.*, 2016, **45**, 6488–6519.

4 E. Díez-Mato, F. C. Cortezón-Tamarit, S. Bogialli, D. García-Fresnadillo and M. D. Marazuela, *Appl. Catal. B Environ.*, 2014, **160–161**, 445–455.

5 M. Magaraggia, F. Faccenda, A. Gandolfi and G. Jori, *J. Environ. Monit.*, 2006, **8**, 923.

6 A. A. Ghogare and A. Greer, *Chem. Rev.*, 2016, **116**, 9994–10034.

7 Y. Liu, T. Pauloehrl, S. I. Presolski, L. Albertazzi, A. R. A. Palmans and E. W. Meijer, *J. Am. Chem. Soc.*, 2015, **137**, 13096–13105.

8 S. Pramual, K. Lirdprapamongkol, J. Svasti, M. Bergkvist, V. Jouan-Hureaux, P. Arnoux, C. Frochot, M. Barberi-Heyob and N. Niamsiri, *J. Photochem. Photobiol. B*, 2017, **173**, 12–22.

9 Q. Zhou, L. Xu, F. Liu and W. Zhang, *Polymer*, 2016, **97**, 323–334.

10 X.-H. Dai, H. Jin, S.-S. Yuan, J.-M. Pan, X.-H. Wang, Y.-S. Yan, D.-M. Liu and L. Sun, *J. Polym. Res.*, , DOI:10.1007/s10965-014-0412-9.

11 Y. Sun, H. Hu, N. Zhao, T. Xia, B. Yu, C. Shen and F.-J. Xu., *Biomaterials*, 2017, **117**, 77–91.

12 C. Li, F. Lin, W. Sun, F.-G. Wu, H. Yang, R. Lv, Y.-X. Zhu, H.-R. Jia, C. Wang, G. Gao and Z. Chen, *ACS Appl. Mater. Interfaces*, 2018, **10**, 16715–16722.

13 L. Wang, J. Li, W. Zhang, G. Chen, W. Zhang and X. Zhu, *Polym. Chem.*, 2014, **5**, 2872–2879.

14 S. Belali, A. R. Karimi and M. Hadizadeh, *Polymer*, 2017, **109**, 93–105.

15 S. Belali, A. R. Karimi and M. Hadizadeh, *Int. J. Biol. Macromol.*, 2018, **110**, 437–448.

16 S. Belali, H. Savoie, J. M. O'Brien, A. A. Cafolla, B. O'Connell, A. R. Karimi, R. W.

Boyle and M. O. Senge, *Biomacromolecules*, 2018, **19**, 1592–1601.

17 E. C. Blossey, D. C. Neckers, A. L. Thayer and A. Paul. Schaap, *J. Am. Chem. Soc.*, 1973, **95**, 5820–5822.

18 F. Prat and C. S. Foote, *Photochem. Photobiol.*, 1998, **67**, 626–627.

19 M. I. Burguete, F. Galindo, R. Gavara, S. V. Luis, M. Moreno, P. Thomas and D. A. Russell, *Photochem. Photobiol. Sci.*, 2009, **8**, 37–44.

20 M. I. Burguete, R. Gavara, F. Galindo and S. V. Luis, *Catal. Commun.*, 2010, **11**, 1081–1084.

21 V. Fabregat, M. I. Burguete, S. V. Luis and F. Galindo, *RSC Adv*, 2017, **7**, 35154–35158.

22 M. Suzuki, Y. Ohta, H. Nagae, T. Ichinohe, M. Kimura, K. Hanabusa, H. Shirai and D. Wohrle, *Chem. Commun.*, 2000, 213–214.

23 S. M. Ribeiro, A. C. Serra and A. M. D. Rocha Gonsalves, *J. Catal.*, 2008, **256**, 331–337.

24 S. Ribeiro, A. C. Serra and A. M. d'A. Rocha Gonsalves, *ChemCatChem*, 2013, **5**, 134–137.

25 J. L. Bourdelande, M. Karzazi, L. E. Dicelio, M. I. Litter, G. Marqués Tura, E. San Román and V. Vinent, *J. Photochem. Photobiol. Chem.*, 1997, **108**, 273–282.

26 J. M. Tobin, T. J. D. McCabe, A. W. Prentice, S. Holzer, G. O. Lloyd, M. J. Paterson, V. Arrighi, P. A. G. Cormack and F. Vilela, *ACS Catal.*, 2017, 4602–4612.

27 E. M. Barker and J. P. Buchanan, *Polymer*, 2016, **92**, 66–73.

28 D. Cambié, C. Bottecchia, N. J. W. Straathof, V. Hessel and T. Noël, *Chem. Rev.*, 2016, **116**, 10276–10341.

29 K. Mizuno, Y. Nishiyama, T. Ogaki, K. Terao, H. Ikeda and K. Kakiuchi, *J. Photochem. Photobiol. C Photochem. Rev.*, 2016, **29**, 107–147.

30 C. Y. Park, Y. J. Kim, H. J. Lim, J. H. Park, M. J. Kim, S. W. Seo and C. P. Park, *RSC*

Adv., 2015, **5**, 4233–4237.

31 C. Mendoza, N. Emmanuel, C. A. Páez, L. Dreesen, J.-C. M. Monbaliu and B. Heinrichs, *ChemPhotoChem*, 2018, **2**, 890–897.

32 E. Boix-Garriga, B. Rodríguez-Amigo, O. Planas and S. Nonell, in *Singlet Oxygen: Applications in Biosciences and Nanosciences*, Nonell, S.; Flors, C., Royal Society of Chemistry, Cambridge, Royal Society of Chemistry., 2016, vol. 1, pp. 23–46.

33 P. R. Ogilby, *Chem. Soc. Rev.*, 2010, **39**, 3181.

34 C. Schweitzer and R. Schmidt, *Chem. Rev.*, 2003, **103**, 1685–1758.

35 R. C. R. Wootton, R. Fortt and A. J. de Mello, *Org. Process Res. Dev.*, 2002, **6**, 187–189.

36 K. Landfester, *Macromol. Rapid Commun.*, 2001, **22**, 896–936.

37 C. S. Chern, *Prog. Polym. Sci.*, 2006, **31**, 443–486.

38 Y. Shiraishi, Y. Kimata, H. Koizumi and T. Hirai, *Langmuir*, 2008, **24**, 9832–9836.

39 P. Kodlekere, A. L. Cartelle and L. A. Lyon, *RSC Adv*, 2016, **6**, 31619–31631.

40 H. J. Hah, G. Kim, Y.-E. K. Lee, D. A. Orringer, O. Sagher, M. A. Philbert and R. Kopelman, *Macromol. Biosci.*, 2011, **11**, 90–99.

41 F. Wilkinson, W. P. Helman and A. B. Ross, *J Phys Chem Ref Data*, 1993, **22**, 113–262.

42 M. Nowakowska, M. Kepczynski and K. Szczubialka, *Pure Appl. Chem.*, 2001, **73**, 491–495.

43 C. Boussiron, M. Le Bechec, L. Petrizza, J. Sabalot, S. Lacombe and M. Save, *Macromol. Rapid Commun.*, 2018, 1800329.

44 F. Amat-Guerri, J. M. Botija and R. Sastre, *J. Polym. Sci. Part Polym. Chem.*, 1993, **31**, 2609–2615.

45 R. T. Gephart, P. N. Coneski and J. H. Wynne, *ACS Appl. Mater. Interfaces*, 2013, **5**,

10191–10200.

46 A. Aluigi, G. Sotgiu, A. Torreggiani, A. Guerrini, V. T. Orlandi, F. Corticelli and G. Varchi, *ACS Appl. Mater. Interfaces*, 2015, **7**, 17416–17424.

47 D. P. Ferreira, D. S. Conceição, R. C. Calhelha, T. Sousa, R. Socoteanu, I. C. F. R. Ferreira and L. F. Vieira Ferreira, *Carbohydr. Polym.*, 2016, **151**, 160–171.

48 F. van Laar, F. Holsteyns, I. F. J. Vankelecom, S. Smeets, W. Dehaen and P. A. Jacobs, *J. Photochem. Photobiol. -Chem.*, 2001, **144**, 141–151.

49 S. Tamagaki and R. Akatsuka, *Bull. Chem. Soc. Jpn.*, 1982, **55**, 3037–3038.

50 J. Gigault, H. El Hadri, S. Reynaud, E. Deniau and B. Grassl, *Anal. Bioanal. Chem.*, 2017, **409**, 6761–6769.

51 J. Gigault, E. Mignard, H. E. Hadri and B. Grassl, *Chromatographia*, 2017, **80**, 287–294.

52 M. J. Barandiaran, J. C. de la Cal and J. M. Asua, in *Polymer Reaction Engineering*, John Wiley & Sons, Ltd, 2008, pp. 233–272.

53 BASF, Safety Data Sheet Vinyl caprolactam Kerobit, 2018.

54 L. Etchenausia, A. Khoukh, E. D. Lejeune and M. Save, *Polym. Chem.*, 2017, **8**, 2244–2256.

55 L. Etchenausia, A. M. Rodrigues, S. Harrisson, E. Deniau Lejeune and M. Save, *Macromolecules*, 2016, **49**, 6799–6809.

56 A. Kermagoret, C.-A. Fustin, M. Bourguignon, C. Detrembleur, C. Jérôme and A. Debuigne, *Polym. Chem.*, 2013, **4**, 2575–2583.

57 D. Crespy, S. Zuber, A. Turshatov, K. Landfester and A.-M. Popa, *J. Polym. Sci. Part Polym. Chem.*, 2012, **50**, 1043–1048.

58 J. M. Asua, *Prog. Polym. Sci.*, 2014, **39**, 1797–1826.

59 T. Hoare and R. Pelton, *J. Phys. Chem. B*, 2007, **111**, 11895–11906.

60 D. Neckers, *J. Photochem. Photobiol. -Chem.*, 1989, **47**, 1–29.

61 O. Valdes-Aguilera and D. C. Neckers, *J. Phys. Chem.*, 1988, **92**, 4286–4289.

62 M. Nowakowska, M. Kepczyński and M. Dabrowska, *Macromol. Chem. Phys.*, 2001, **202**, 1679–1688.

63 H. B. Rodríguez, E. S. Román, P. Duarte, I. F. Machado and L. F. Vieira Ferreira, *Photochem. Photobiol.*, 2012, **88**, 831–839.

64 D. K. Luttrull, O. Valdes-Aguilera, S. M. Linden, J. Paczkowski and D. C. Neckers, *Photochem. Photobiol.*, 1988, **47**, 551–557.

65 M. E. Rodriguez, V. E. Diz, J. Awruch and L. E. Dicelio, *Photochem. Photobiol.*, 2010, **86**, 513–519.

66 J. Paczkowski and D. C. Neckers, *J. Photochem.*, 1986, **35**, 283–287.

67 J. Paczkowski and D. C. Neckers, *Macromolecules*, 1985, **18**, 2412–2418.